Available online at www.sciencedirect.com
SCIENCE DIRECT
Biochemical Pharmacology 69 (2005) 627–634
Biochemical Pharmacology
www.elsevier.com/locate/biochempharm

Determination of the potency and subunit-selectivity of ribonucleotide reductase inhibitors with a recombinant-holoenzyme-based in vitro assay

Jimin Shao[a,b], Bingsen Zhou[a], Lijun Zhu[a,b], Angel J. Di Bilio[c], Leila Su[d], Yate-Ching Yuan[d], Shijun Ren[e], Eric J. Lien[e], Jennifer Shih[a], Yun Yen[a,*]

[a]*Department of Medical Oncology and Therapeutic Research, City of Hope National Medical Center, Duarte, CA 91010, USA*
[b]*Department of Basic Medical Sciences, Zhejiang University School of Medicine, Hangzhou, Zhejiang 310031, PR China*
[c]*Department of Chemistry, California Institute of Technology, Pasadena, CA 91125, USA*
[d]*Department of Bioinformatics, City of Hope National Medical Center, Duarte, CA 91010, USA*
[e]*Department of Pharmaceutical Sciences, School of Pharmacy, University of Southern California, Los Angeles, CA 90089, USA*

Received 16 September 2004; accepted 9 November 2004

Abstract

Ribonucleotide reductase (RR) is an important therapeutic target for anticancer drugs. The structure of human RR features a 1:1 complex of two homodimeric subunits, hRRM1 and hRRM2. p53R2 is a newly identified homologue of hRRM2. We have devised a holoenzyme-based in vitro assay for the determination of the potency and subunit-selectivity of small-molecule inhibitors of RR. The assay was implemented using two forms of recombinant RR (hRRM2/hRRM1 and p53R2/hRRM1) and based on their [^{3}H]CDP reduction activity. Hydroxyurea was used to standardize the assay. We found that the activities of hRRM2/hRRM1 and p53R2/hRRM1 were decreased by hydroxyurea in a dose-dependent manner. The –NH–OH segment of hydroxyurea was shown to be essential for inhibition. In the presence of Fe(III) and reductants, less inhibition of enzymatic activity by hydroxyurea was observed, especially for p53R2/hRRM1. The potency of four hydroxyurea analogues (Schiff bases of hydroxysemicarbazide, SB-HSC) decreased in the order SB-HSC 21 > SB-HSC 24 > SB-HSC 2 > hydroxyurea (HU) > SB-HSC 29. SB-HSC 2 and SB-HSC 24 inhibited p53R2/hRRM1 significantly more than hRRM2/hRRM1, whereas SB-HSC 21 and SB-HSC 29 showed low subunit-selectivity. Electron paramagnetic resonance (EPR) measurements showed that inhibition of RR was accompanied by reduction of its tyrosyl radical. The method was validated by comparison with data obtained using cell-based assays. We suggest that this novel recombinant-holoenzyme-based in vitro assay is a useful tool for the discovery of more potent and subunit-selective inhibitors of RR.

Keywords: Ribonucleotide reductase inhibitors; Potency and subunit-selectivity; In vitro assay; Two forms of holoenzyme; Recombinant subunit proteins

1. Introduction

Ribonucleotide reductase (RR) catalyzes the conversion of the four ribonucleotides to deoxyribonucleotides, which are required for DNA synthesis. The human enzyme is a class I RR whose quaternary structure features a 1:1 complex of two homodimeric subunits, hRRM1 and hRRM2 [1,2]. p53R2 is a newly identified hRRM2 homologue (81.2% amino acid sequence identity) that is regulated by the tumor suppressor p53 protein [3,4]. hRRM1 harbors the catalytic site, allosteric effector sites, and redox active disulfides. hRRM2 contains an oxygen-linked binuclear iron cluster and a stable tyrosyl radical. A long-range proton-coupled electron-transfer pathway between the small and large subunits is central for function [5,6]. The 9 GHz EPR (electron paramagnetic resonance) spectra of *Escherichia coli*, mouse, and human RRs are similar, thereby indicating that in all three enzymes, the dihedral

Abbreviations: RR, ribonucleotide reductase; HU, hydroxyurea; SC, semicarbazide; SB-HSCs, Schiff bases of hydroxysemicarbazide; KB-$_{WT}$, KB wild-type cells; KB-$_{HUR}$, KB HU-resistant cells; EPR, electron paramagnetic resonance; QSAR, quantitative structure–activity relationship; DTT, dithiothreitol

* Corresponding author. Tel.: +1 626 359 8111x62307; fax: +1 626 301 8233.
E-mail address: yyen@coh.org (Y. Yen).

0006-2952/$ – see front matter © 2004 Elsevier Inc. All rights reserved.
doi:10.1016/j.bcp.2004.11.016

angle between the C_β–H bond and the axis perpendicular to the aromatic ring of the tyrosyl radical are close [7–9]. The in vitro activities of hRRM2/hRRM1 and p53R2/hRRM1 depend on the integrity of both the dinuclear iron center and tyrosyl radical [9–11]. It has been suggested that hRRM2/hRRM1 supplies dNTPs for DNA replication in a cell cycle-dependent manner, whereas p53R2/hRRM1 supplies dNTPs for DNA repair in a p53-dependent manner [12–18].

Ribonucleotide reductase is an important target for anticancer drugs because of its key role in the early events of tumor development; the enzyme is directly involved in tumor growth, metastasis, and drug resistance [19–23]. Therefore, small-molecule inhibitors of RR have been widely investigated as potential anti-tumoral chemotherapeutic agents. Strategies for inhibition of the enzyme include quenching of the tyrosyl radical, disruption of the dinuclear iron center, use of nucleoside analogues to inhibit the large subunit, and perturbation of critical interactions between subunits. The RR inhibitor hydroxyurea (HU) has been marketed for cancer therapy for the past 30 years [19]. HU blocks DNA synthesis by reducing the tyrosyl radical and perturbing the iron center of the enzyme [24–26]. The deoxycytidine analogue Gemcitabine (its diphosphate metabolite directly inhibits RR) has recently been approved for treatment of pancreatic cancer and non-small cell lung cancer [27]. Triapine (a new small-molecule RR inhibitor) is in phase II clinical trials [28]. The discovery of p53R2 raises important questions, as this protein could be a target in cancer therapy. Because hRRM2 and p53R2 play different roles in cells, inhibitors specific for each subunit may exhibit different clinical values [12]. Specific inhibition of hRRM2 is a potential therapeutic strategy to kill cancer cells. Upon DNA damage, cancer cells often cannot induce p53R2 due to the lack of p53, whereas normal cells can repair their DNA with help from induced p53R2. Thus, use of genotoxic chemotherapeutic agents in combination with hRRM2 inhibitors is an attractive treatment plan [18,29]. On the other hand, inhibitors specific for p53R2 may be useful for targeting tumors that overexpress p53R2, because its inhibition increases the sensitivity of cells to DNA damaging agents [3,13,24,30]. In cells that retain the p53 wild-type gene, it is expected that inactivation of p53R2-dependent DNA synthesis would activate p53-dependent apoptosis [3,12,13].

We reported the syntheses and anti-proliferation properties of 30 Schiff bases of hydroxysemicarbazide (SB-HSC) that bear the pharmacophore –NH–OH identified in HU [31,32]. The anti-tumoral activity and structure of these compounds was correlated by quantitative structure–activity relationship (QSAR) analysis [32,33]. In this work, we report a new holoenzyme-based in vitro assay using two forms of human RR (hRRM2/hRRM1 and p53R2/hRRM1) reconstituted from recombinant subunits. HU, semicarbazide (SC), and four HU derivatives (SB-HSCs 2, 21, 24, and 29) were chosen as test compounds (Fig. 1). These four structurally diverse SB-HSCs showed the strongest inhibition of tumor cell growth among 30 tested Schiff bases of hydroxysemicarbazide. The well-characterized RR inhibitor HU was used as standard and positive control. SC, which is inactive in cell-based assay, was used as negative control. The method is validated by electron paramagnetic resonance (EPR) measurements and by comparison with data obtained in cell proliferation assays. Our findings may contribute to the discovery of novel anticancer agents that are potent and subunit-selective inhibitors of RR.

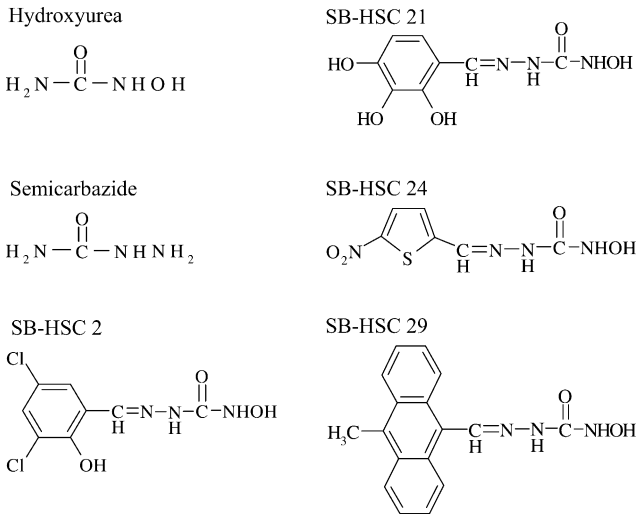

Fig. 1. Structures of hydroxyurea, semicarbazide, and Schiff bases of hydroxysemicarbazide.

2. Materials and methods

2.1. Chemicals

Hydroxyurea (Sigma), DMSO (Sigma), and semicarbazide (Aldrich) were used as purchased. SB-HSC 2, SB-HSC 21, SB-HSC 24, and SB-HSC 29 were kindly provided by Dr. Lien (Department of Pharmaceutical Sciences, School of Pharmacy, University of Southern California).

2.2. Preparation of recombinant proteins

The coding sequences of hRRM2, p53R2, and hRRM1 were obtained from human oropharyngeal carcinoma KB wild-type cells (KB-$_{WT}$) (ATCC) and cloned in-frame with a N-terminal 6× His-tag into the prokaryotic expression vector pET28 (Novagen). The proteins were expressed in BL21 (DE3) bacteria (Stratagene) and purified using Ni(II) affinity chromatography (Qiagen) [9]. The purified proteins (in 50 mM Tris–HCl, pH 7.4, 100 mM KCl) were stored at −70 °C. Protein concentration was measured with a protein assay kit (Bio-Rad). Protein purity was determined by densitometric scanning of the coomassie-stained SDS–PAGE gel.

2.3. In vitro RR assay

HU and SC were dissolved in water. The SB-HSCs were dissolved in neat DMSO and diluted with deionized water. The final concentration of DMSO in the reaction mixtures was 1% (v/v) for SB-HSC 21, and 2.5% (v/v) for SB-HSC 2, SB-HSC 24, and SB-HSC 29. The enzymatic activity of RR in the crude extracts of mammalian cells was measured using the Steeper and Stuart CDP reductase activity method [21,34]. The method was modified and standardized for assaying the potency and subunit-selectivity of the inhibitors using purified recombinant RR subunits as follows. Step 1: a mixture of purified hRRM1 and either hRRM2 or p53R2 was incubated at room temperature for 30 min with various concentrations of each compound. Step 2: to initiate enzymatic reduction, a reaction buffer (0.125 μM [^{3}H] CDP, 50 mM HEPES (pH 7.2), 6 mM DTT, 4 mM MgOAc, 2 mM ATP, 0.05 mM CDP, 100 mM KCl, and 0.24 mM NADPH) was added to the protein and inhibitor mixture from step 1 up to a final volume of 100 μl. Where indicated, up to 60 μM $FeCl_3$ was added to the reaction buffer. The reaction mixture was incubated at 37 °C for 30 min. The enzyme substrate CDP and dCDP formed in the reaction mixture were dephosphorylated using phosphodiesterase. Step 3: the cytidine and deoxycytidine in the reaction mixture were separated by HPLC using a C18 reversed-phase column connected to a Model 2 β-RAM Radio Flow-Through detector (IN/US Systems). Negative control samples, which were run with each experiment, only contained 1 or 2.5% (v/v) DMSO. The extent of enzyme inhibition was expressed as a percentage of the negative control (relative activity). The relative enzyme activity dependence on inhibitor concentration was fitted using a non-linear regression equation $(f(x) = (a - d)/[1 + (x/c)^b] + d$, where a = asymptotic maximum, b = slope parameter, c = value at the inflection point, and d = asymptotic minimum). The IC_{50} values, namely the compound's concentration that produces 50% inhibition, were calculated by setting $f(x) = 50$. The inhibitory potency is reported as the mean (±S.D.) of three separate tests, each performed in duplicate. The significance of the data was determined using the Student's t-test (two-tail). $p < 0.05$ was deemed significant.

2.4. Cell lines and cell proliferation assay

KB-$_{WT}$ cells were cultured in RPMI 1640 supplemented with 10% (v/v) fetal bovine serum in a 5% CO_2 humidified atmosphere at 37 °C. KB HU-resistant cells (KB-$_{HUR}$) were selected in a stepwise manner in the presence of HU, cloned, and maintained under a selection pressure of 1 mM HU [21]. The resistant cells were grown in drug-free medium for 48 h prior to use. KB-$_{WT}$ and KB-$_{HUR}$ cells in logarithmic growth were seeded at a density of 50,000 cells/ml in 24-well plates. After 24 h, solutions of HU, SC, and SB-HSCs (prepared as described above) were added to cells for cytotoxicity determination. Cultures were incubated for 72 h and subsequently methylene blue assays were performed [21]. The IC_{50} values (50% cell death) were determined using eight different concentrations of each compound. The concentration of DMSO in the cell cultures was 1% (v/v) for the initial (highest) compound concentration and the corresponding control.

2.5. Electron paramagnetic resonance (EPR) spectroscopy

EPR measurements were conducted on purified hRRM2 and p53R2. The protein samples were incubated with each compound at room temperature for 30 min and then flash-frozen using liquid nitrogen. Control samples did not contain inhibitor. EPR spectra were recorded with a Bruker EMX spectrometer equipped with an Oxford helium cryostat. Instrumental parameters: microwave frequency = 9.376 GHz, microwave power = 0.5 mW, modulation amplitude 4 G (100 kHz), and sample temperature = 10 K.

3. Results

3.1. Assay development using recombinant RR subunits

Recombinant hRRM2, p53R2, and hRRM1 were prokaryotically expressed and isolated in a single chromatographic step to about 90% purity (Fig. 2). hRRM2 and p53R2 were separately mixed with hRRM1 to give active holoenzymes. To optimize the quantity of protein employed in the assay, hRRM2 and p53R2 were titrated against various concentrations of hRRM1. For a standard assay, RR was reconstituted by mixing 0.5 μM hRRM1 (∼4.5 μg) with 1 μM hRRM2 or p53R2 (∼4.5 μg). Using a smaller amount of hRRM1 relative to hRRM2 and p53R2

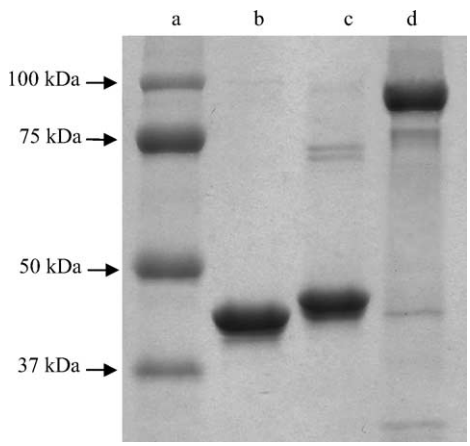

Fig. 2. Ten percent SDS–PAGE analyses of recombinant hRRM1, hRRM2, and p53R2. (a) Molecular mass marker; (b) p53R2 (42 kDa, 3 μg); (c) hRRM2 (45 kDa, 3 μg); and (d) hRRM1 (90 kDa, 5 μg).

increased the activity comparability between the two small subunits. The specific enzymatic activities determined under standard assay conditions were 72.5 ± 2.62 nmol of dCDP/min/mg for hRRM2 and 50.6 ± 2.25 nmol of dCDP/min/mg for p53R2. The sample volume is 100 μl and the assay can be run in multiple-well plates. The assay includes three steps: (1) incubation of the test compound with holoenzyme, (2) initiation of the enzymatic reaction, and (3) detection of activity. The first and second steps take about 2 h; at least 100 samples can be analyzed every 24 h by an HPLC-isotope detector set (third step).

3.2. Assay standardization using hydroxyurea

HU inhibited hRRM2/hRRM1 and p53R2/hRRM1 in a concentration-dependent manner. Importantly, up to 5 mM SC did not significantly inhibit RR (Fig. 3A). To assess the effect of iron on activity, the reaction buffer was supplemented with $FeCl_3$. The Fe(III) salt had little effect on the activities of hRRM2/hRRM1 and p53R2/hRRM1. However, $FeCl_3$ affected the potency of HU (Fig. 3B). In the absence of $FeCl_3$, the HU IC_{50} values (Table 1) are 165 ± 7.95 μM for hRRM2/hRRM1 and 190 ± 6.43 μM for p53R2/hRRM1, indicating a slight preference toward hRRM2/hRRM1 ($p < 0.05$). Notably, in the presence of $FeCl_3$, the HU IC_{50} value increased by nearly an order of magnitude for p53R2/hRRM1 (1990 ± 71.2 μM), whereas a more modest increase was measured for hRRM2/hRRM1 (556 ± 24.1 μM). For simplicity, all the in vitro RR assays described below were conducted in the absence of $FeCl_3$.

3.3. Effect of DMSO

DMSO is the most commonly used solvent for hydrophobic compounds in biological assays. High concentrations of DMSO caused significantly greater inhibition of p53R2/hRRM1 over hRRM2/hRRM1 (Fig. 3C). To investigate the effect of DMSO on the potency of HU, hRRM2/hRRM1 and p53R2/hRRM1 were exposed to increasing concentrations of HU dissolved in 1% (v/v) of DMSO. By itself, this low concentration of DMSO had no significant effect on inhibition of hRRM2/hRRM1. However, DMSO increased the sensitivity of p53R2/hRRM1 to HU, lowering the HU IC_{50} to a value similar to that for hRRM2/hRRM1 ($p > 0.05$, Fig. 3D). A second set of experiments were conducted using 2.5% (v/v) DMSO. Increasing the concentration of DMSO from 1 to 2.5% had no significant effect on the IC_{50} values of HU for either hRRM2/hRRM1 or p53R2/hRRM1 ($p > 0.05$) (Table 1).

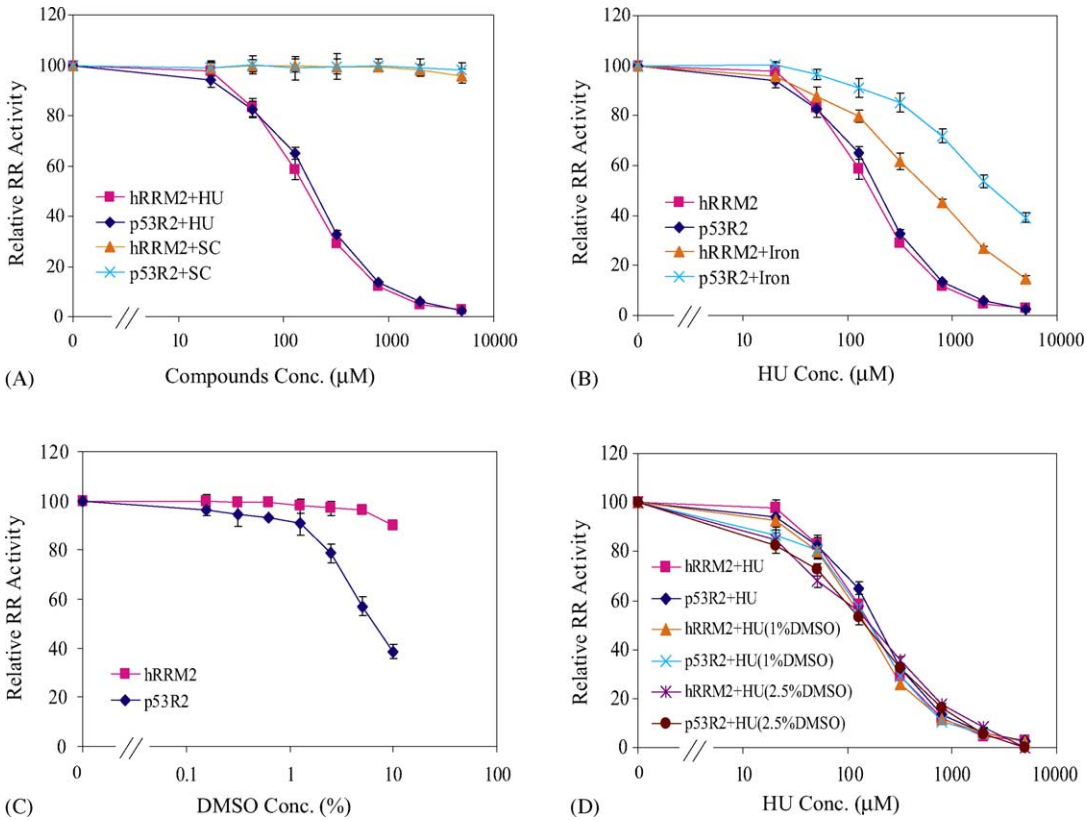

Fig. 3. Effects of hydroxyurea, semicarbazide, and DMSO on the activities of hRRM2/hRRM1 and p53R2/hRRM1. (A) Dependence of the enzyme activities on HU and SC. (B) Activities of enzyme samples supplemented with $FeCl_3$, DTT, and NADPH as a function of HU concentration. (C) Activities of enzyme samples as a function of DMSO percentage (the DMSO percentage was varied by serial two-fold dilutions of 10% DMSO down to 0.156% (v/v)). (D) Activities of enzyme samples as a function of HU concentration with 1 and 2.5% DMSO (v/v). The concentration of inhibitor in (A), (B), and (D) was varied by serial 2.5-fold dilutions of 5000 μM inhibitor down to 20.4 μM). Each data point is the mean ± S.D. of three separate experiments (each in duplicate).

Table 1
Potency and subunit-selectivity of HU and SB-HSCs

Compound	$IC_{50} \pm$ S.D. (μM)[a]		Average potency[b]	Subunit-selectivity[c]
	hRRM2/hRRM1	p53R2/hRRM1		
SC (in dH_2O)	>5000	>5000	>5000	NA
HU (in dH_2O)	165 ± 7.95	190 ± 6.43	178	0.868
HU (in dH_2O + $FeCl_3$)	556 ± 24.1	1990 ± 71.2	1270	0.279
HU (in 1% DMSO)	148 ± 7.34	159 ± 6.82	153	0.931
HU (in 2.5% DMSO)	155 ± 6.59	146 ± 6.06	150	1.06
SB-HSC2 (in 2.5% DMSO)	111 ± 6.64	30.6 ± 1.62	70.7	3.62
SB-HSC21 (in 1% DMSO)	11.5 ± 0.630	13.6 ± 0.700	12.5	0.847
SB-HSC24 (in 2.5% DMSO)	52.0 ± 2.03	11.5 ± 0.600	31.7	4.53
SB-HSC29 (in 2.5% DMSO)[d]	>250	>250	>250	NA

[a] IC_{50} is the concentration of the compounds producing 50% inhibition of the reconstituted RR activity. Values are the mean ± S.D. of three separate experiments, each performed in duplicate.
[b] [IC_{50} (hRRM2) + IC_{50} (p53R2)]/2.
[c] IC_{50} (hRRM2)/IC_{50} (p53R2).
[d] The maximum solubility of SB-HSC 29 in 2.5% DMSO was 250 μM. At this concentration of SB-HSC 29, RR was inhibited <50%, which corresponds to an $IC_{50} > 250$ μM.

3.4. Determination of potency and subunit specificity of SB-HSCs

The IC_{50} values for HU and the SB-HSCs determined using the in vitro RR assay are set out in Table 1. For both small subunits, the inhibitory potency decreased in the order SB-HSC 21 > SB-HSC 24 > SB-HSC 2 > HU > SB-HSC 29. SB-HSC 2 and SB-HSC 24 were significantly more efficient at inactivating p53R2, with subunit-selectivity indices of 3.62 and 4.53, respectively (Fig. 4). SB-HSC 21 showed almost no preference for either subunit (subunit-selectivity index 0.847). The IC_{50} values of SB-HSC 29 with both hRRM2 and p53R2 were >250 μM.

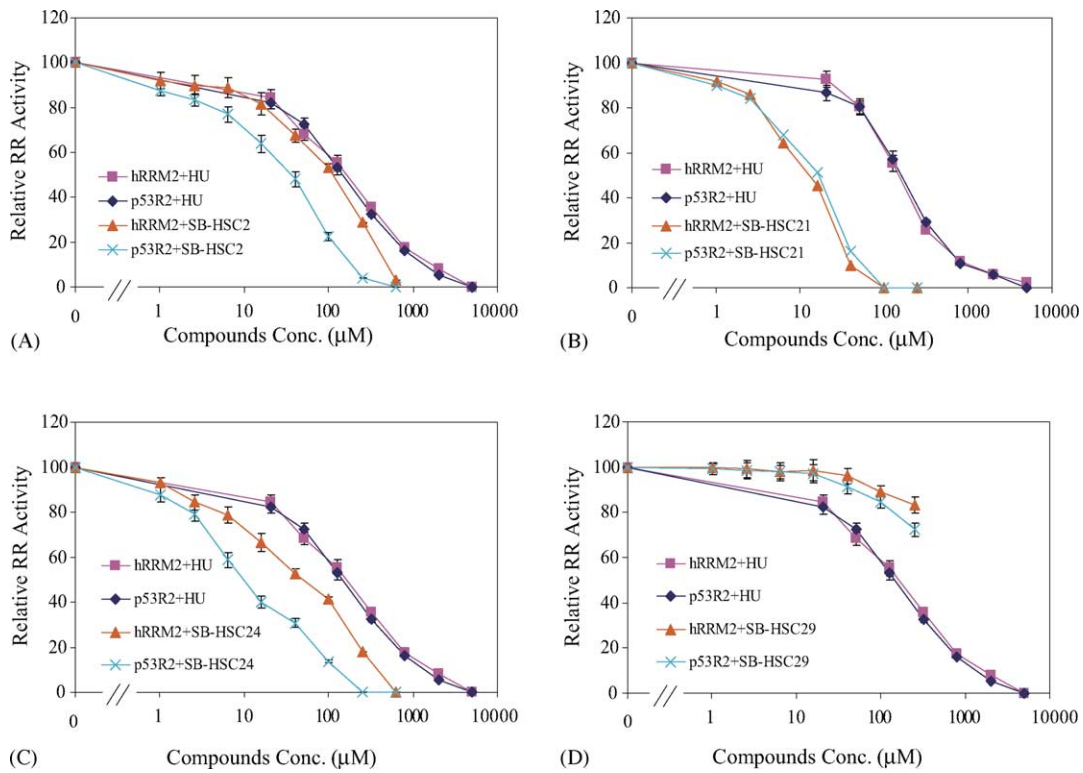

Fig. 4. Comparison of potency and subunit-selectivity of HU and SB-HSCs. Samples of hRRM2/hRRM1 and p53R2/hRRM1 were incubated with the SB-HSCs and assayed. The concentration of the inhibitors was varied; the inhibitor concentration was varied by serial 2.5-fold dilutions (the initial concentration of inhibitor was 625 μM except for SB-HSC 29 for which it was 250 μM). SB-HSC 21 was dissolved in 1% (v/v) DMSO; SB-HSCs 2, 24, and 29 were dissolved in 2.5% (v/v) DMSO. Solutions of HU in 1 and 2.5% (v/v) DMSO was used as control. Each data point is the mean ± S.D. of three separate experiments (each in duplicates).

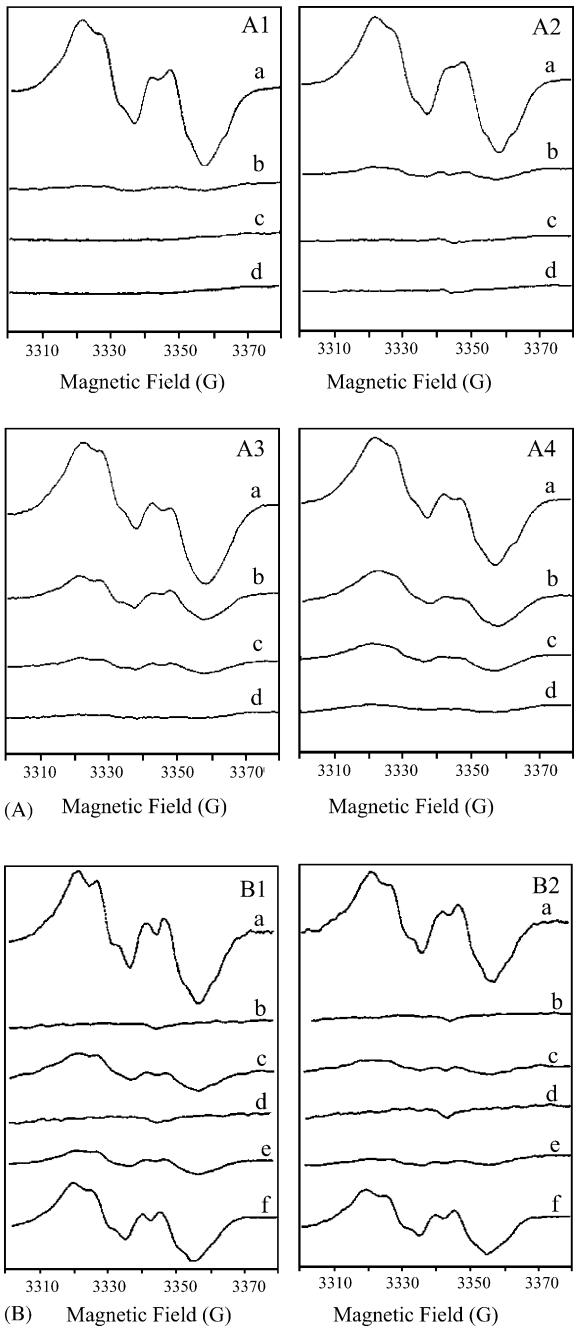

Fig. 5. Quenching and regeneration of the stable tyrosyl radical of hRRM2 and p53R2. (A) EPR spectra of frozen solutions containing 120 μg/150 μl of hRRM2 (A1, A3) and p53R2 (A2, A4). The protein samples were incubated with HU at 25 °C for 30 min and then flash-frozen in liquid nitrogen (A1, A2); or incubated with HU at 25 °C for 30 min, and then supplemented with $FeCl_3$, DTT, and NADPH and incubated at 37 °C for another 30 min (A3, A4). *a*, dH_2O (control); *b*, 0.625; *c*, 1.25; and *d*, 2.5 mM HU. (B) EPR spectra of frozen solutions containing 80 μg/120 μl of hRRM2 (B1) and p53R2 (B2). The protein samples were incubated with SB-HSCs at 25 °C for 30 min and then flash-frozen in liquid nitrogen. *a*, 2.5% (v/v) DMSO (negative control); *b*, 2.5 mM HU (positive control); *c*, SB-HSC 2; *d*, SB-HSC 21; *e*, SB-HSC 24; and *f*, SB-HSC 29 (the concentration of the SB-HSCs was 250 μM).

Table 2
Cytotoxicity of HU and SB-HSCs

Compound	$IC_{50} \pm$ S.D. (μM)[a]		
	KB-$_{WT}$	KB-$_{HUR}$	L1210[b]
SC	>10000	>10000	>2192
HU	455 ± 16.2	6750 ± 37.5	82.0 ± 6.0
SB-HSC2	22.2 ± 2.10	21.2 ± 1.52	6.5 ± 0.6
SB-HSC21	37.5 ± 5.20	15.3 ± 1.71	2.7 ± 0.6
SB-HSC24	27.2 ± 0.290	28.0 ± 1.56	10.6 ± 0.3
SB-HSC29	9.25 ± 0.590	8.88 ± 0.653	4.4 ± 0.0

[a] IC_{50} is the concentration of the compounds producing 50% inhibition of cell growth. Values are the mean ± S.D. of three separate experiments, each performed in duplicate.

[b] IC_{50} values observed in the murine leukemia cell line L1210 (from [32]).

3.5. Cytotoxicity assay

The inhibitory activities of HU and the SB-HSCs against human oropharyngeal carcinoma KB-$_{WT}$ and KB-$_{HUR}$ cells were determined using cell proliferation assays (Table 2). The SB-HSCs showed higher inhibitory activities than HU but no cross-resistance with HU. The cytotoxicity results are comparable with the average potency of the test compounds for both small subunits obtained using the in vitro RR assay, with the exception of SB-HSC 29.

3.6. Reduction and regeneration of the tyrosyl radical

EPR measurements were conducted on samples of hRRM2 and p53R2 that were treated with HU and the SB-HSCs. Reduction of the tyrosyl radical (which was indicated by a lower intensity of the EPR signal relative to that for untreated protein) in both small subunits by incubation with HU occurred in a dose-dependent manner (Fig. 5A). Quenching of the tyrosyl radical by HU, however, was partially reversed upon further incubation with $FeCl_3$, DTT, and NADPH. The yield of tyrosyl radical regeneration was higher for p53R2. Without HU treatment, $FeCl_3$ and the reductants had little effect on the intensity of the EPR signals. The EPR measurements also show that the SB-HSCs quenched the tyrosyl radical of both small subunits (Fig. 5B). The intensities of the EPR signals are consistent with the effect of the inhibitors on enzymatic activity. SB-HSC 29 was the least effective radical scavenger.

4. Discussion

Among current strategies for drug discovery, recombinant protein and cell-based screening assays use functional and mechanism-related approaches [35–37]. We have presented a simple in vitro assay suitable for the determination of the potency and subunit-selectivity of RR inhibitors. The method was implemented using highly purified recombinant proteins and optimized by tightly controlling the ratio

of the subunits in the reaction mixture, the composition of the reaction buffer, and the concentration of DMSO solvent. The procedure was adapted for the examination of a large number of compounds in a short time. The potency and subunit specificity of small molecules is measured directly and quantitatively by using two RRs, hRRM2/hRRM1 and p53R2/hRRM1.

Binding affinity and specificity, which are largely dependent on the molecular structure and physicochemical properties of a drug, are important determinants of drug activity. HU, SC, and four SB-HSCs were chosen to test the in vitro assay because they have different structures and antitumoral activities (Fig. 1). The potencies of these compounds decrease in the order SB-HSC 21 > SB-HSC 24 > SB-HSC 2 > HU > SB-HSC 29, in accordance with data measured in this and a previous report using cell proliferation assays [31,32]. Because of its small size and hydrophilic nature, HU may easily diffuse within a protein matrix. However, HU has low binding specificity, which limits its efficacy [32,38,39]. Specific structural features of the SB-HSCs significantly enhance their anti-tumor activity. QSAR analyses suggest that the hydrophobic ring and electron-rich substituents at the *ortho*- and *meta*-positions may explain the higher pharmacological activities of SB-HSC 2, SB-HSC 21, and SB-HSC 24 [32,33]. The halogenated phenyl group of SB-HSC 2 may favor steric interactions that could enhance binding affinity to protein. The phenolic groups of SB-HSC 21 could function as free radical scavengers and increase its potency. The higher potency of SB-HSC 24 is probably related to the strong electron-withdrawing effect of the nitrothienyl group. The –NH–OH segment of HU and the SB-HSCs is absent in the substantially inactive SC. We infer that the –NH–OH group is the minimal structural requirement that triggers inhibition of RR enzymatic activity. SB-HSC 2 and SB-HSC 24 showed selectivity for p53R2/hRRM1 over hRRM2/hRRM1. This was confirmed by EPR measurements on samples of p53R2 and hRRM2 that were treated with these two compounds. It is likely that the physicochemical properties of the SB-HSCs and structural differences between the small subunits interplay to promote subunit-selectivity. SB-HSC 29 behaved poorly, both as a tyrosyl radical quencher and activity inhibitor, which was unexpected because SB-HSC 29 exerts potent growth-inhibition of cell lines (Table 2) [31,32]. Because of its larger size and highly hydrophobic anthracene ring, SB-HSC 29 might act via a different mechanism of action in vivo. In cells, SB-HSC 29 could target other proteins or be metabolized to cytotoxic products. The basic condition for the generation of a model by any QSAR method is that the tested compounds have the same molecular target. Thus, protein-based assays are superior to cell-based assays for QSAR analysis.

Samples of hRRM2 and p53R2 yielded strong EPR signals, which mean that protein integrity is maintained in our preparations. This is attributable to the use of a mild one-step chromatographic procedure for protein isolation.

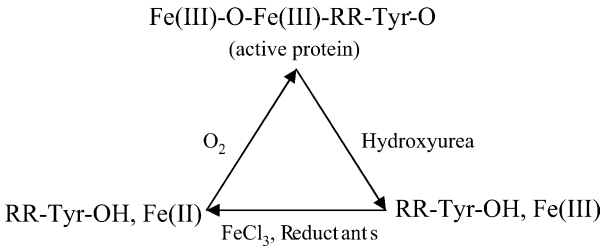

Fig. 6. Schematic diagram of the reduction and regeneration of hRRM2 and p53R2.

A correlation between inhibition of RR and reduction of its tyrosyl radical has been demonstrated [5]. Our EPR data clearly shows that HU and the SB-HSCs quench the tyrosyl radical. Radical reduction and disruption of the dinuclear iron cluster results in formation of apo-RR (protein lacking the dinuclear iron cluster and stable tyrosyl radical). In vitro regeneration of mouse apo-R2 (mouse R2 is the counterpart of hRRM2) is carried out by incubating protein under aerobic conditions with an Fe(II) salt in the presence of reducing agents [5,40]. We have shown that after exposure to HU, the tyrosyl radicals of hRRM2 and p53R2 are partially reformed by addition of $FeCl_3$, DTT, and NADPH (Fig. 5). The reductants, which are present in the assay reaction buffer, prevent oxidation of the –SH group of hRRM1. In addition, they reduce Fe(III), making Fe(II) available for the regeneration reaction (Fig. 6). Less inhibition of enzymatic activity and less reduction of the tyrosyl radical by HU occurs for p53R2 in the presence of Fe(III) and reductants, indicating that the tyrosyl radical of p53R2 is more easily regenerated than that of hRRM2. The selectively of HU for hRRM2/hRRM1 over p53R2/hRRM1 is remarkable. Since cells have both, an iron pool and reductants, it is likely that HU will inhibit hRRM2 in vivo more than p53R2.

We have devised a useful in vitro assay for screening novel inhibitors of RR using two forms of the enzyme reconstituted with recombinant subunits. Moreover, the assay is a powerful tool for investigation of the mechanism of action of RR inhibitors. Better understanding of the factors that promote subunit specificity in small-molecule inhibitors and the importance of structural differences between p53R2 and hRRM2 could offer new perspectives for the rational design of cancer chemotherapeutic agents that target ribonucleotide reductase.

Acknowledgements

We thank Dr. Melissa Holtz and Rhea Harris-Junge for insightful comments.

References

[1] Reichard P. From RNA to DNA, why so many ribonucleotide reductases? Science 1993;260:1773–7.

[2] Stubbe J, Van Der Donk WA. Protein radicals in enzyme catalysis. Chem Rev 1998;98:705–62.
[3] Tanaka H, Arakawa H, Yamaguchi T, Shiraishi K, Fukuda S, Matsui K, et al. A ribonucleotide reductase gene involved in a p53-dependent cell-cycle checkpoint for DNA damage. Nature 2000;404:42–9.
[4] Nakano K, Balint E, Ashcroft M, Vousden KH. A ribonucleotide reductase gene is a transcriptional target of p53 and p73. Oncogene 2000;19:4283–9.
[5] Gräslund A. Ribonucleotide reductase: kinetic methods for demonstrating radical transfer pathway in protein R2 of mouse enzyme in generation of tyrosyl free radical. Methods Enzymol 2002;354:399–414.
[6] Chang MC, Yee CS, Stubbe J, Nocera DG. Turning on ribonucleotide reductase by light-initiated amino acid radical generation. Proc Natl Acad Sci USA 2004;101:6882–7.
[7] Pesavento RP, van der Donk WA. Tyrosyl radical cofactors. Adv Protein Chem 2001;58:317–85.
[8] Svistunenko DA, Cooper CE. A new method of identifying the site of tyrosyl radicals in proteins. Biophys J 2004;87:582–95.
[9] Shao J, Zhou B, Zhu L, Qiu W, Yuan YC, Xi B, et al. In vitro characterization of enzymatic properties and inhibition of the p53R2 subunit of human ribonucleotide reductase. Cancer Res 2004;64:1–6.
[10] Kauppi B, Nielsen BB, Ramaswamy S, Larsen IK, Thelander M, Thelander L, et al. The three-dimensional structure of mammalian ribonucleotide reductase protein R2 reveals a more-accessible iron-radical site than *Escherichia coli* R2. J Mol Biol 1996;262:706–20.
[11] Stubbe J. Di-iron-tyrosyl radical ribonucleotide reductases. Curr Opin Chem Biol 2003;7:183–8.
[12] Lozano G, Elledge SJ. p53 sends nucleotides to repair DNA. Nature 2000;404:24–5.
[13] Yamaguchi T, Matsuda K, Sagiya Y, Iwadate M, Fujino MA, Nakamura Y, et al. p53R2-dependent pathway for DNA synthesis in a p53-regulated cell cycle checkpoint. Cancer Res 2001;61:8256–62.
[14] Guittet O, Hakansson P, Voevodskaya N, Fridd S, Gräslund A, Arakawa H, et al. Mammalian p53R2 protein forms an active ribonucleotide reductase in vitro with the R1 protein, which is expressed both in resting cells in response to DNA damage and in proliferating cells. J Biol Chem 2001;276:40647–51.
[15] Kimura T, Takeda S, Sagiya Y, Gotoh M, Nakamura Y, Arakawa H. Impaired function of p53R2 in Rrm2b-null mice causes severe renal failure through attenuation of dNTP pools. Nature Genet 2003;34:440–5.
[16] Xue L, Zhou B, Liu X, Qiu W, Jin Z, Yen Y. Wild-type p53 regulates human ribonucleotide reductase by protein-protein interaction with p53R2 as well as hRRM2 subunits. Cancer Res 2003;63:980–6.
[17] Zhou B, Liu X, Mo X, Xue L, Darwish D, Qiu W, et al. The human ribonucleotide reductase subunit hRRM2 complements p53R2 in response to UV-induced DNA repair in cells with mutant p53. Cancer Res 2003;63:6583–94.
[18] Lin ZP, Belcourt MF, Cory JG, Sartorelli AC. Stable suppression of the R2 subunit of ribonucleotide reductase by R2-targeted siRNA sensitizes p53 (−/−) HCT-116 colon cancer cells to DNA-damaging agents and ribonucleotide reductase inhibitors. J Biol Chem 2004;279:27030–8.
[19] Nocentini G. Ribonucleotide reductase inhibitors: new strategies for cancer chemotherapy. Crit Rev Oncol Hematol 1996;22:89–126.
[20] Fan H, Villegas C, Huang A, Wright JA. The mammalian ribonucleotide reductase R2 component cooperates with a variety of oncogenes in mechanisms of cellular transformation. Cancer Res 1998;58:1650–3.
[21] Yen Y, Grill SP, Dutschman GE, Chang CN, Zhou BS, Cheng YC. Characterization of a hydroxyurea-resistant human KB cell line with supersensitivity to 6-thioguanine. Cancer Res 1994;54:3686–91.
[22] Zhou BS, Hsu NY, Pan BC, Doroshow JH, Yen Y. Overexpression of ribonucleotide reductase in transfected human KB cells increases their resistance to hydroxyurea: M2 but not M1 is sufficient to increase resistance to hydroxyurea in transfected cells. Cancer Res 1995;55:1328–33.
[23] Zhou BS, Tsai P, Ker R, Tsai J, Ho R, Yu J, et al. Overexpression of transfected human ribonucleotide reductase M2 subunit in human cancer cells enhances their invasive potential. Clin Exp Metastasis 1998;16:43–9.
[24] Le NT, Richardson DR. The role of iron in cell cycle progression and the proliferation of neoplastic cells. Biochim Biophys Acta 2002;1603:31–46.
[25] Lassmann G, Thelander L, Gräslund A. EPR stopped-flow studies of the reaction of the tyrosyl radical of protein R2 from ribonucleotide reductase with hydroxyurea. Biochem Biophys Res Commun 1992;188:879–87.
[26] Nyholm S, Thelander L, Gräslund A. Reduction and loss of the iron center in the reaction of the small subunit of mouse ribonucleotide reductase with hydroxyurea. Biochemistry 1993;32:11569–74.
[27] Goan YG, Zhou B, Hu E, Mi S, Yen Y. Overexpression of ribonucleotide reductase as a mechanism of resistance to 2,2-difluorodeoxycytidine in the human KB cancer cell line. Cancer Res 1999;59:4204–7.
[28] Yen Y, Margolin K, Doroshow J, Fishman M, Johnson B, Clairmont C, et al. A phase I trial of 3-aminopyridine-2-carboxaldehyde thiosemicarbazone in combination with gemcitabine for patients with advanced cancer. Cancer Chemother Pharmacol 2004;54:331–42.
[29] Eklund H, Uhlin U, Farnegardh M, Logan DT, Nordlund P. Structure and function of the radical enzyme ribonucleotide reductase. Prog Biophys Mol Biol 2001;77:177–268.
[30] Yanamoto S, Kawasaki G, Yoshitomi I, Mizuno A. Expression of p53R2, newly p53 target in oral normal epithelium, epithelial dysplasia and squamous cell carcinoma. Cancer Lett 2003;190:233–43.
[31] Ren S, Tokes ZA, Csipke C, Zhou B, Yen Y, Lien EJ. Inhibition of tumor cell growth by Schiff bases of hydroxysemicarbazide. Anticancer Res 2001;21:3445–51.
[32] Ren S, Wang R, Komatsu K, Bonaz-Krause P, Zyrianov Y, McKenna CE, et al. Synthesis, biological evaluation, and quantitative structure–activity relationship analysis of new Schiff bases of hydroxysemicarbazide as potential antitumor agents. J Med Chem 2002;45:410–9.
[33] Raichurkar AV, Kulkarni VM. Understanding the antitumor activity of novel hydroxysemicarbazide derivatives as ribonucleotide reductase inhibitors using CoMFA and CoMSIA. J Med Chem 2003;46:4419–27.
[34] Steeper JP, Stuart CD. A rapid assay for CDP reductase activity in mammalian cell extracts. Anal Biochem 1970;34:123–30.
[35] Workman P. The opportunities and challenges of personalized genome-based molecular therapies for cancer: targets, technologies, and molecular chaperones. Cancer Chemother Pharmacol 2003;52:45–56.
[36] Kirkpatrick P. Virtual screening, different routes to the same answer. Nature Rev Drug Discov 2003;2:947.
[37] Torrance CJ, Agrawal V, Vogelstein B, Kinzler KW. Use of isogenic human cancer cells for high-throughput screening and drug discovery. Nat Biotechnol 2001;19:940–5.
[38] Larsen IK, Sjöberg BM, Thelander L. Characterization of the active site of ribonucleotide reductase of *Escherichia coli*, bacteriophage T4 and mammalian cells by inhibition studies with hydroxyurea analogues. Eur J Biochem 1982;125:75–81.
[39] Nordlund P, Sjöberg BM, Eklund H. Three-dimensional structure of the free radical protein of ribonucleotide reductase. Nature 1990;345:593–8.
[40] Ochiai E, Mann GJ, Gräslund A, Thelander L. Tyrosyl free radical formation in the small subunit of mouse ribonucleotide reductase. J Biol Chem 1990;265:15758–61.